Metabolomics of biofluids : from analytical tools to data interpretation

Nevedomskaya, E.

Chapter 4

Metabolic Profiling of Accelerated Aging ERCC1$^{d/-}$ Mice

Nevedomskaya E., Meissner A., Goraler S., de Waard M., Ridwan Y., Zondag G., van der Pluijm I., Deelder A.M, Mayboroda O.A.

Journal of Proteome Research **2010**, 9, 3680–3687

ABSTRACT

Aging is a fundamental biological process for which the mechanism is still largely unknown due to its complex and multifactorial nature. Animal models allow us to simplify this complexity and to study individual factors separately. As there are many causative links between DNA repair deficiency and aging, we studied the ERCC1$^{d/-}$ mouse, which has a modified ERCC1 gene, involved in the Nucleotide Excision Repair, and as a result has a premature aging phenotype. Profiling of these mice on different levels can give an insight into the mechanisms underlying the aging phenotype. In the current study, we have performed metabolic profiling of serum and urine of these mice in comparison to wild type and in relation to aging by ^{1}H NMR spectroscopy. Analysis of metabolic trajectories of animals from 8 to 20 weeks suggested that wild type and ERCC1$^{d/-}$ mutants have similar age-related patterns of changes; however, the difference between genotypes becomes more prominent with age. The main differences between these two genetically diverse groups of mice were found to be associated with altered lipid and energy metabolism, transition to ketosis, and attenuated functions of the liver and kidney.

INTRODUCTION

Aging is a complex biological process that involves multiple systems at different regulation levels. Understanding of its mechanisms will allow better understanding of the impairment of human health that occurs at old age.(1) Despite many efforts, the etiology of aging is still largely unknown. It is evident that it cannot be explained by a single or a couple of mechanisms but rather by a complex network of interdependent processes involved.

Several theories have been proposed for mechanisms of aging, one of them being "free radical theory of aging".(2;3) According to this theory, free radicals represent the greatest danger for DNA, which is the blueprint for all genes and therefore RNAs and proteins. If DNA is irreversibly damaged, this has severe consequences for human health, which is illustrated by several human inherited DNA repair deficient disorders, which all show signs of premature aging. Examples of these diseases are Trichothiodystrophy and Cockayne syndrome, which both bear mutations in genes involved in nucleotide excision repair (NER) and as a result develop a plethora of premature aging symptoms including, but not limited to, neuronal problems, growth retardation, vision and hearing impairment, and a greatly reduced lifespan.(4) This illustrates the importance of DNA repair and hints at the fact that unrepaired DNA damage results in an aging phenotype.

Due to its complex nature and the time involved to develop the phenotype, aging is difficult to study in humans. A possible alternative is the use of animal models such as mice, nematodes, and others.(5) The ERCC1$^{-/-}$ mouse with a single gene knockout in nucleotide excision repair system is one of such model animals.(6) The ERCC1 gene encodes a protein that is part of an endonuclease complex essential for both NER and interstrand cross-link repair (ICLR).(7) These mutant mice have a significantly reduced lifespan of up to 4 weeks only and a severe premature aging phenotype with a range of features including aging-like skin abnormalities, reduced growth, liver and kidney dysfunction, as well as others.(8) This extremely short lifetime makes it difficult to monitor the progression of aging, and the highly anomalous phenotype does not only reflect fast aging. The ERCC1$^{d/-}$ mouse combines knockout of ERCC1 in one allele and a truncated ERCC1 allele (9) and helps to overcome those extreme effects, as this delays the display of symptoms of aging and prolongs the lifespan. The resulting phenotype shows premature aging features such as neurological problems, impaired vision and hearing, growth retardation, a shortened lifespan of about 6 months (as compared to 2.5/3 years for a wild type mouse), and also accumulation of somatic mutations.(10)

ERCC1$^{d/-}$ mice aging phenotype is expected to be reflected in the composition of biofluids. This can be the subject of investigation by proteomics, glycomics, or metabolomics. The latter is of particular interest as it is focused on studying small

molecules that are end-points of biochemical processes and can give insight into changes happening in the whole organism.(11;12)

One of the established methods in metabolomics is nuclear magnetic resonance (NMR), which allows measurement and recovery of molecular information over a wide range of small compounds.(13;14)

Two main questions arise with regard to metabolic profiling of ERCC1$^{d/-}$ mice. The first one is how different the metabolome of a particular biofluid of the mutant mice is from that of the wild type. The other one is how the metabolic profiles change with aging of ERCC1$^{d/-}$ animals in general and in comparison to changes that occur in normal mice. These questions imply that the experimental design should include both mutants and wild type mice as well as follow the same animals to monitor metabolic changes with aging in a longitudinal design. To answer these types of questions on the basis of NMR, data multivariate statistical analysis tools (*e.g.*, Principal Component Analysis, Partial Least Squares *etc.*) are needed.(15;16)

In the current study, we have analyzed cohorts of serum and urine samples from wild type and ERCC1$^{d/-}$ mutant mice by ^{1}H NMR and have detected compounds that differ between the groups as well as specific age-related changes. The biological significance of these findings is discussed.

MATERIALS AND METHODS

Sample Collection. Experiments were performed in accordance with the "Principles of laboratory animal care" (NIH publication no. 86-23) and the guidelines approved by the Erasmus University animal care committee. The generation of ERCC1^{-} and ERCC1^{d} alleles has been previously described.(9) ERCC1$^{d/-}$ mice were obtained by crossing ERCC1^{-} with ERCC1$^{d/+}$ mice of C57Bl6J and FVB backgrounds to yield ERCC1$^{d/-}$ with C57Bl6J/FVB hybrid background. Wild-type littermates were used as controls. Mice were housed in individual ventilated cages with ad libitum access to standard mouse food (CRM pellets, SDS BP Nutrition Ltd.; gross energy content 18.36 kJ/g dry mass, digestible energy 13.4 kJ/g) and water. Food intake was measured for animals individually; no difference for the studied group of ERCC1$^{d/-}$ mutants compared to wild type animals was observed for the studied age group relative to the body weight (table with body weights of groups of animals, Supplementary Materials, Table S1).

Longitudinal serum samples were collected from 20 animals, 10 wild type and 10 ERCC1$^{d/-}$ mutants, gender matched, at 4 time points - 8, 12, 16, and 20 weeks. Blood was collected via extraction from the tail vein, after which serum was collected by centrifugation at 6000 rpm and the supernatant was transferred to a fresh tube and stored at -70 °C. A few

samples were missing or had too small a volume, so that the total number of samples measured was 70.

Urine samples were collected from 13 wild type animals and from 13 ERCC1$^{d/-}$ mutants, with unbiased selection of gender and age between 8 and 16 weeks. Urine of animals was collected on a piece of Parafilm between 11.00 and 13.00 h for each mouse and stored at -70 °C.

Blood glucose was measured using a Freestyle mini blood glucose measurement device (Abbott Diabetes Care).

NMR Sample Preparation. For sample preparation, buffer was added to all samples to reduce variability in pH and supply a deuterated lock solvent. The specific buffers for urine and serum are described below.

For serum preparation, 60 µL of 75 mM phosphate buffer in H_2O/D_2O (80/20) at pH 7.4 containing 6.15 mM NaN_3 and 4.64 mM sodium 3-[trimethylsilyl] d4-propionate (TSP) was added to 20 µL of serum and manually transferred into Bruker 1.7 mm NMR Match tubes.

For urine preparation, 40 µL of 0.20 M phosphate buffer in D_2O at pH 7.0 containing 0.26 mM NaN_3 and 0.53 mM TSP was added to 40 µL urine and manually transferred into Bruker 1.7 mm NMR Match tubes.

NMR Spectroscopy. All NMR experiments were acquired on a 600 MHz Bruker Avance II spectrometer (Bruker BioSpin, Karlsruhe, Germany) equipped with a 5 mm TCI cryogenic probe head with Z-gradient system and automatic tuning and matching. Temperature calibration was done prior to each batch of measurements using the method of Findeisen *et al.*(17)

For urine, one-dimensional ^{1}H NMR spectra were recorded at 300 K using the first increment of a NOESY (18) pulse sequence with presaturation (γB_1 = 50 Hz) during a relaxation delay of 4 s and a mixing time of 10 ms for efficient water suppression. A total of 32 768 data points were recorded with 32 scans covering a sweep width of 12336 Hz. The free induction decay (FID) was zero-filled to 65 536 complex data points prior to Fourier transformation and an exponential window function was applied with a line broadening factor of 1.0 Hz.

For serum, 1D NOESY and 1D diffusion edited(19) experiments were recorded at 310 K. Presaturation with an effective field of 50 Hz during a relaxation delay of 4 s was applied and a total of 98 304 data points were recorded covering a sweep width of 18 029 Hz for both experiments. For 1D NOESY, a total of 32 scans were accumulated with water resonance saturation (γB_1 = 50 Hz) during a mixing time of 10ms. For the diffusion edited 1D experiment, a gradient echo delay of 116 ms was utilized and a total of 64 scans were recorded for each sample. For both experiments, the FID was zero-filled to 131 072 complex

data points prior to Fourier transformation and an exponential window function was applied with a line broadening factor of 1.0 Hz. All spectra were manually phase and baseline corrected using Topspin 2.1 (Bruker BioSpin, Karlsruhe, Germany) and automatically referenced to TSP (0.0 ppm).

Data Analysis. Each spectrum was integrated using 0.04 ppm integral regions between 11 and -1 ppm, excluding the residual water region in serum spectra from 5.0 to 4.6 ppm, the residual water and urea region in urine spectra from 5.0 to 4.7 ppm and from 6.2 to 5.6 ppm respectively, and the TSP signal from 0.025 to -0.025 in both sets of spectra. The citrate region in urine spectra was integrated using spectral regions from 2.76 to 2.66 ppm and from 2.60 to 2.52 ppm to avoid effects introduced by positional noise of the peaks due to differences in ion strength and pH between the samples. To account for any difference in concentration between samples, each spectrum was normalized to its total area.

Data sets were imported into SIMCA-P+ 12.0 (Umetrics, Umeå, Sweden) to perform multivariate statistics: principal component analysis (PCA) and partial least squares discriminant analysis (PLS-DA). The partial least squares (PLS) method was used for analysis of time changes in spectra with aging of the animals. Pareto scaling was used for all the statistical models.

Identification of metabolites was facilitated by using the Statistical Total Correlation Spectroscopy (STOCSY) approach (20) using in-house developed routines written in R statistical language (http://www.r-project.org/). This method determines and visualizes correlations between peaks in sets of NMR spectra, allowing annotation of peaks belonging to the same molecule. Annotation of peaks was performed based on reference spectra from the Bruker Bioref database (Bruker BioSpin, Karlsruhe, Germany).

For visualization of differentially expressed metabolites, spectra were aligned using the COW algorithm (21) and averaged.

For glucose quantification, all non-normalized spectra were referenced to the doublet in the anomeric region. Quantification was performed by deconvolution and subsequent integration of glucose anomeric signal (5.25-5.22 ppm) using an in-house developed automation routine (see Supplementary Materials). The absolute concentrations were calculated based on internal reference TSP with correction for TSP protein binding and line-broadening effects.

RESULTS

Profiling of Serum Metabolites in ERCC1$^{d/-}$ Mice by ^{1}H NMR. PCA analysis of the integrated (binned) NOESY data reflects both effects of genotype (differences between wild type and mutants) (Figure 1A) and age-related differences (Figure 1B). The first two

principal components cover more than 65% of the variation and reflect these biological processes. No gender-related separation was observed.

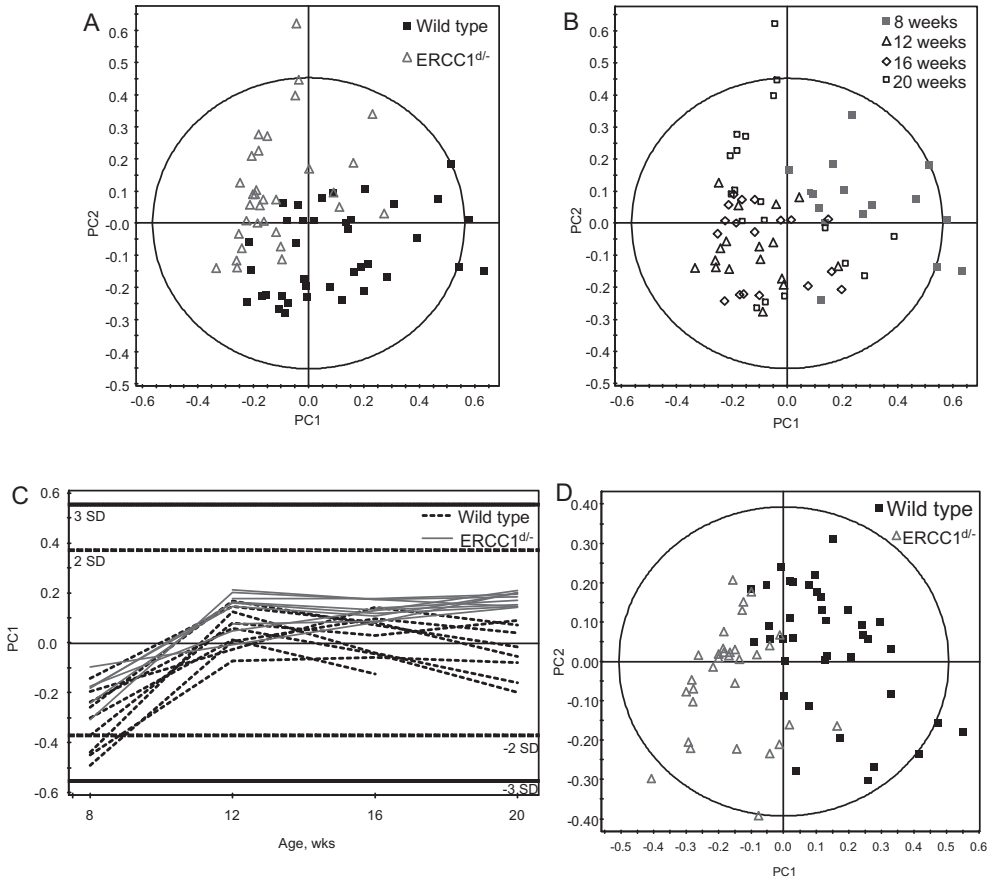

Figure 1. Multivariate statistical analysis of serum NMR data. (A) PCA scores plot, wild type (■) and ERCC1$^{d/-}$mutant mice (Δ). (B) PCA scores plot, 8 weeks (■), 12 (Δ), 16 (◊) and 20 (□) weeks mouse samples. (C) Batch PLS scores plot of serum samples mapped across the different ages. Dashed horizontal lines show two and three standard deviations for the data set. Dashed lines represent wild type, grey lines represent ERCC1$^{d/-}$ mutants. (D) PLS-DA scores plot (for first two principal components R2Y = 60.3%, Q2 = 56.9%) showing discrimination between wild type (■) and ERCC1$^{d/-}$mutant mice (Δ).

The PCA scores plot (Figure 1B) shows that profiles of both mutants and controls at 8 weeks considerably differ from profiles at other ages. Dependence on the age was studied using PLS batch analysis; the clear trend on the age could only be seen along the first

principal component (Figure 1C), while along the other components variation is not related to the lifetime. Compounds associated with the age component were found to be mainly related to lipids and lipoproteins (Supplementary Materials, Figure S1).

In addition, Figure 1C shows that while at 8 and 12 weeks there is overlap between wild type and mutant animals along the first component, at 16 weeks they start to separate and at 20 weeks mutant animals are completely distinct from the wild type and show less intragroup variation. This observation was also confirmed by building separate PLS-DA models at all four ages. The separation efficiency and model quality increased with age; the explained variation of the response variable (R2Y) values for the models were from 50% at 8 weeks to 87% at 20 weeks, while the variation of the response variable predicted by the model (Q2) increased from 10% to 80%.

Further investigation of the differences between wild type animals and mutants and identification of the molecular discriminators was performed using a PLS-DA model built with the genotype as response variable (Figure 1D). Model validation using permutation test showed a good fit and validity of the model (Supplementary Materials, Figure S2). Spectral regions responsible for separation of the two groups were selected on the basis of VIP values (variable importance in the projection); variables with values over 1.5 were selected. The identity of the underlying compounds was investigated based on the chosen spectral regions. However, identification of chemical structures based only on a single peak that falls into a specified bin interval can be difficult. To assist annotation of key discriminators, the STOCSY approach was used. In this method correlations between a selected peak and all other peaks in the spectra are explored and visualized; peaks characterized by high correlations belong to the same molecule and can be confidently annotated using reference spectra (Supplementary Materials, Figure S4).

As can be seen from Table 1, most of the compounds responsible for separation of mutant mice from wild type are related to lipoprotein distribution and concentrations and some of these regions were also found to be associated with age trajectories.

In addition to changes in the lipid profile, lactate is decreased and alanine is increased. Averaged spectra from both of the groups with selected compounds highlighted are shown in Figure 2.

Investigation of the line shapes of diffusion edited spectra in the region of aliphatic CH_3 and CH_2 lipid resonances allows us to estimate relative changes of different classes of lipoproteins.(22) The differences in the lipid region between the two groups indicate that ERCC1$^{d/-}$ mutants show an increased level of high density lipoproteins (HDL) and a decreased level of low and very low density lipoproteins (LDL and VLDL respectively) compared to wild type (Figure 3).

Table 1. Integrated regions (bins), which show different concentrations between serum profiles of wild type and mutant animals.

spectral region, ppm	fold change[a]	identity	p-value[b]
1.52-1.48	1.1	Alanine	4.81E-12
0.68-0.64	1.14	Unidentified	2.11E-10
1.6-1.56	-1.15	Lipid **CH$_2$**CH$_2$CO	1.53E-09
2.28-2.24	-1.24	Lipid **CH$_2$**CO	2.13E-09
2.08-2.04	-1.16	N-acetyl glycoproteins	3.84E-09
1.12-1.08	1.09	Unidentified	6.62E-09
0.92-0.88	-1.21	Lipoproteins	1.93E-08
1.56-1.52	1.08	Unidentified	2.41E-08
1.32-1.28	-1.49	Lipid $(CH_2)_n$	3.89E-08
0.88-0.84	1.18	Lipoproteins	8.65E-08
1.36-1.32	-1.28	Lactate	1.90E-07
3.24-3.2	1.3	Choline $-N(CH_3)_3$	1.09E-06
1.4-1.36	-1.16	Lipoproteins	1.46E-06
2.12-2.08	-1.05	Unidentified	1.67E-06
5.36-5.32	-1.34	Unsaturated lipids	5.89E-06
1.24-1.2	1.16	Lipoproteins	1.57E-05
2-1.96	1.05	Lipid	5.33E-05
1.28-1.24	1.16	Lipoproteins	5.64E-05
4.16-4.12	-1.1	Lactate	6.29E-05

[a] Calculated as difference in mean levels in ERCC1$^{d/-}$ mutant relative to wild type animals. The + and - indicate the direction of the change, i.e. - for reduced level in ERCC1$^{d/-}$ samples, + for increased level in ERCC1$^{d/-}$ samples compared to wild type.

[b] Unpaired t-test using a Benjamini–Hochberg correction for the p-values.

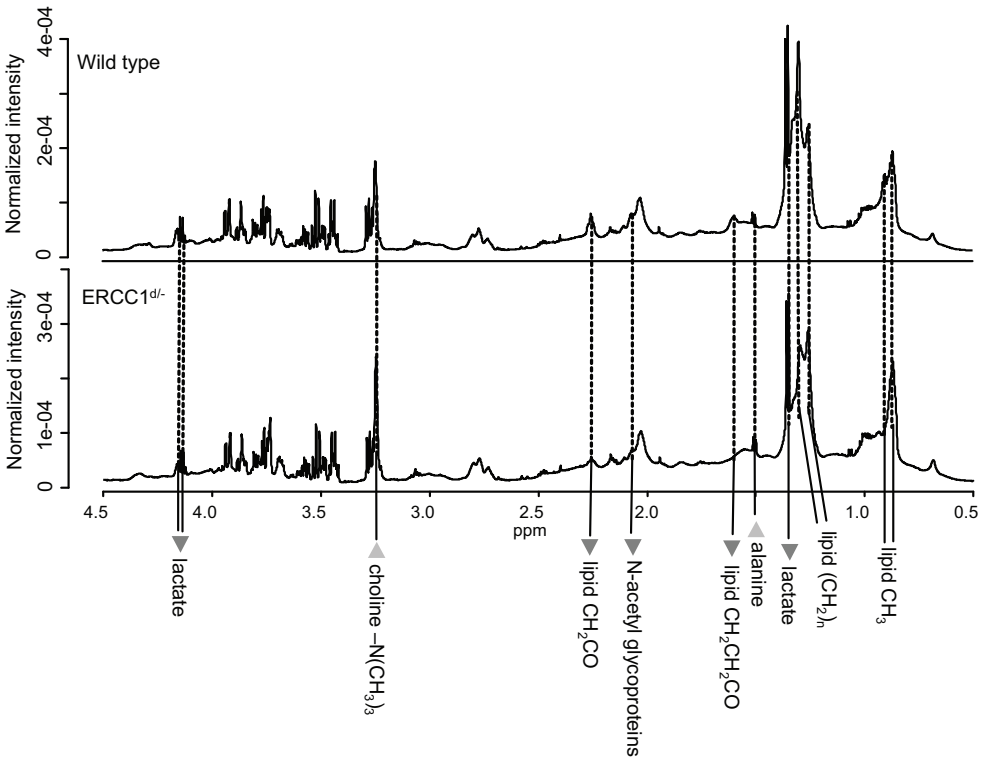

Figure 2. Averaged ^{1}H NMR spectral regions of serum from wild type (above) and ERCC1$^{d/-}$ mutant (below) animals. Differential metabolites are highlighted; ▼stands for down-regulated, ▲ for up-regulated compounds.

Glucose was measured in blood samples by a glucose measurement device (Freestyle mini, Abbott Diabetes Care), and its concentrations were found to be different between the animals with different genetic backgrounds (Supplementary Materials, Figure S5A), p-value obtained by t test is 0.001. However, ppm regions corresponding to glucose did not appear to have an influence in multivariate analysis. The reason for this might be that there are broad signals that overlay the glucose peaks due to high protein content of the samples. That is why proper deconvolution and integration were needed to correctly quantify glucose. Results obtained from NMR data were similar to those received by a conventional method (Supplementary Materials, Figure S5B). The trend was the same: glucose is lower in ERCC1$^{d/-}$ animals than in wild type (p-value obtained by t test is <0.001).

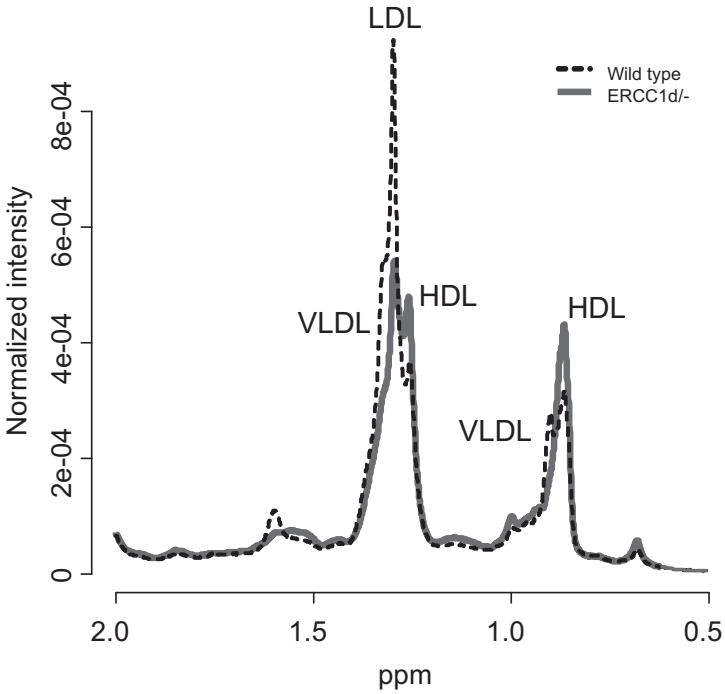

Figure 3. Spectral region corresponding to lipoproteins, averaged diffusion edited spectra of wild type (dashed line), and ERCC1$^{d/-}$mutants animals (grey line).

Profiling of Urine Metabolites in ERCC1$^{d/-}$ Mice by ^{1}H NMR. Global changes in biochemical processes in the organism should be reflected not in one particular biological fluid, such as blood, but should also be seen in others, for instance urine. Longitudinal collection of sufficient quantities of urine from the same animals from which serum was collected was not feasible due to the small size of the mutant animals and difficulties with their urination. However, we performed analysis of urine obtained from a different cohort.

As a first step, a PCA model was built that showed clear separation of wild type animals from ERCC1$^{d/-}$ mutants (Figure 4A). PLS-DA was performed, which gave a very good model with R2Y = 91.7 and Q2 = 85.3% for the first two components. On the basis of this model, variables responsible were identified and annotated (Table 2). The average spectra from both of the groups with these compounds highlighted are shown in Figure 4B. There are other differential signals visible in averaged spectra, but those were not found to be statistically significant.

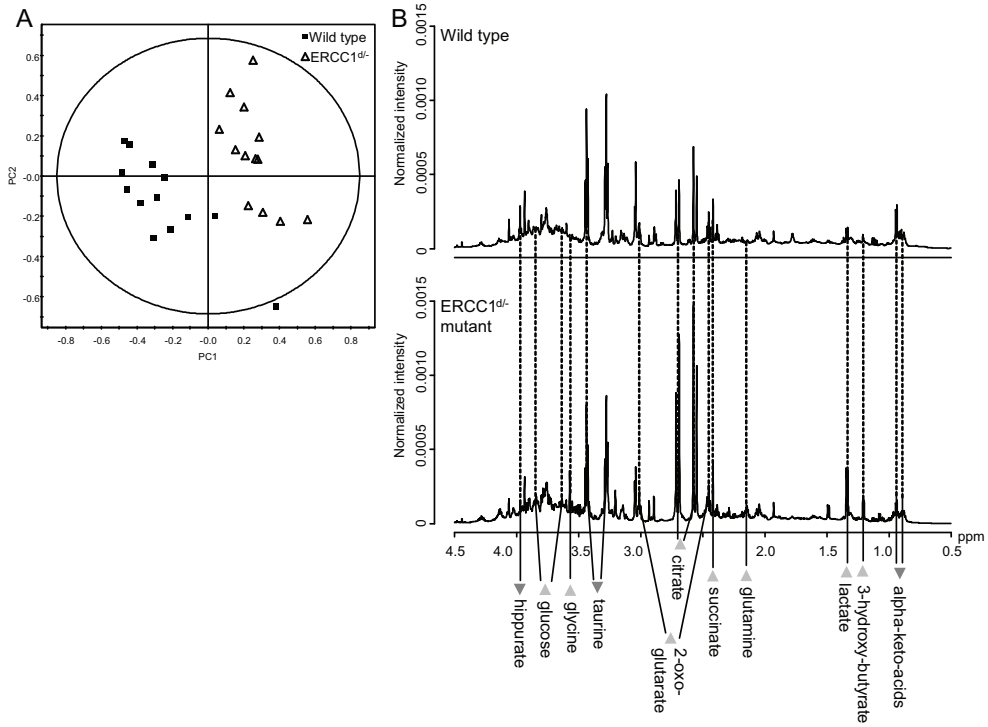

Figure 4. Urine ^{1}H NMR analysis. (A) PCA scores plot on urinary metabolic profiles scores plot, first two principal components cover 35.7% and 23.3% of variability, respectively. Separation between wild type (■) and ERCC1$^{d/-}$ mutant mice (Δ) is visible. (B) Averaged ^{1}H NMR spectral regions of urine samples of wild type (above) and ERCC1$^{d/-}$ mutant (below) animals. Differential metabolites are highlighted; ▼ down-regulated compounds, ▲ up-regulated compounds.

Table 2. Integrated Regions (Bins), which Show Different Concentrations between Urine Profiles of Wild Type and Mutant Animals.

ppm	fold change[a]	identity	p-value[b]
0.96-0.92	-1.56	Alpha-keto acids	7.48E-11
2.64-2.6	-1.59	Ketoleucine	2.08E-10
1.16-1.12	-1.7	Alpha-keto acids	1.60E-09
2.76-2.64	2.18	Citrate	1.60E-05
7.28-7.24	-2.07	Unidentified	4.46E-05
0.92-0.88	-1.49	Alpha-keto acids	5.62E-05
2.6-2.52	2.24	Citrate	9.03E-05
2.16-2.12	1.76	Glutamine	<0.0002
3.24-3.2	1.53	Unidentified	<0.0002
1.36-1.32	2.12	Lactate	0.001
3.56-3.52	1.39	Glucose	0.001
7.56-7.52	-2.51	Hippuric acid	0.001
7.84-7.8	-2.68	Hippuric acid	<0.002
3.28-3.24	1.32	TMAO	0.002
4-3.96	-1.46	Hippuric acid	0.003
3.32-3.28	-1.74	Taurine	0.006
3.52-3.48	1.57	Glucose	0.007
3.6-3.56	1.33	Glycine	0.02
5.4-5.36	-1.19	Allantoin	0.03
2.48-2.44	1.38	2-Oxoglutarate	0.05
2.44-2.4	1.15	Succinate	0.14
1.24-1.2	1.03	3-Hydroxybutyrate	0.43

[a] Calculated as difference in mean levels in ERCC1$^{d/-}$ mutant relative to wild type animals. The + and - indicate the direction of the change, i.e. - for reduced level in ERCC1$^{d/-}$ samples, + for increased level in ERCC1$^{d/-}$ samples compared to wild type.

[b] unpaired t-test using a Benjamini–Hochberg correction for the p-values

DISCUSSION

ERCC1$^{d/-}$ mutant mice represent a model which can provide insight into the biological processes involved in aging.(9) While phenotypic changes that occur in these animals have been characterized before, this is the first study in which the global profiling on the metabolite level was done by NMR.

For both serum and urine, PCA was performed as a first step of data analysis to evaluate the structure present in the data. Unsupervised analysis of ^{1}H NMR serum spectra showed that the major variance in the data matrix reflects two biological phenomena: animal genotype (Figure 1A) and their lifetime (Figure 1B); both are represented with the first two principal components covering together more than 65% of the variation. To explore the effects of those phenomena on metabolic profiles of the body fluids of the animals, supervised methods such as PLS-DA, for example, were employed.

Batch PLS analysis was chosen to explore more in-depth age-related changes. This analysis as well as PCA showed that 8 weeks old mice are considerably different from mice at older age, and this is true for both wild type and mutant mice. This might be due to the fact that at around 10 weeks the maturity of mice sets in and this is expected to involve serious changes in the overall metabolism which are reflected in the NMR spectra. It was also found that the difference between the sample groups is more prominent at older ages, while at younger ages metabolic profiles of mutant and wild type animals are more similar. This fact indicates that ERCC1$^{d/-}$ mutant animals develop more or less normally until the point of a sexual maturity, but begin to exhibit accelerated aging after reaching maturity and hence are a very good model for senescence and biological aging.

The effect of genotype on metabolic composition of serum was studied by PLS-DA which revealed a number of compounds altered between the groups.

Most of the differences in serum between wild type and mutant animals were found to be associated with lipids, either increased or decreased in mutants compared to wild type mice. It has been hypothesized that fast aging mice, which have disruptions in the NER pathway, might have the corresponding adaptive "survival" response of the organism similar to that of caloric restriction.(23;24) In this respect, analysis of the relative changes in lipid and lipoproteins might be of special interest, because in caloric restriction a specific pattern of changes in lipoprotein composition of blood has been shown.(25) Line shapes in the lipoprotein region in diffusion-edited spectra indicate that in ERCC1$^{d/-}$ mutant mice LDL and VLDL are decreased and HDL is increased, and this pattern of changes indeed resembles the state of caloric restriction.

Both the conventional method and NMR-based quantification showed that glucose is decreased in serum of ERCC1$^{d/-}$ mutants compared to wild type (Supplementary Materials, Figure S5). This is another indication for a phenotype that resembles caloric restriction. Low levels of another compound derived from the glucose metabolism, lactate, were observed in serum samples of ERCC1$^{d/-}$ mutants compared to controls; its decrease might be related to a decrease in the Cori cycle.

It is obviously of particular interest to see how the changes in serum are comparable with alterations in urine composition, if any of the biochemical processes reflected in one of the biofluids can as well be seen in the other. Therefore, we performed analysis of urine from a smaller cohort to investigate the involvement of the biochemical processes obtained by serum analysis.

In contrast to serum, glucose and lactate were found to be elevated in urine of mutants compared to wild type animals. Compounds of the TCA cycle: citrate, succinate, and 2-oxoglutarate - also showed higher levels in urine of ERCC1$^{d/-}$ mice compared to wild type animals. These compounds are involved in a large number of biochemical processes, and their alterations are difficult to interpret as they might occur due to a variety of reasons.(26) One of the possible explanations for the observed opposite changes of glucose metabolites in blood and urine is the kidney dysfunction, which leads to an impaired reabsorption of these molecules in renal tubules.(27)

In urine, there is an indication of the altered energy metabolism as well; it was found to be switched to fatty-acids utilization, shown by the presence of 3-hydroxybutyrate, one of the ketone bodies. This compound was found present only in ERCC1$^{d/-}$ mice while in wild type animals there is another unidentified compound present with a singlet in the same region as the doublet of 3-hydroxybutyrate (Supplementary Materials, Figure S6). This would explain the low fold-change value in Table 2 for 3-hydroxybutyrate as the values are calculated for integrated intensities in the binned region. Together with low glucose in blood, the presence of 3-hydroxy-butyrate is an indication of ketosis.(28) in the mutant mice. It is important to note that no difference in food intake relative to the body weight was observed in ERCC1$^{d/-}$ mutants compared to wild type controls. This means that the switch to ketosis in these animals occurs not as a response to food deficiency.

Other compounds observed that might be changing due to ketosis are alpha-keto acids (2-oxo-3-methylbutanoic, and 2-oxo-3-methylpentanoic acids), which can be used in liver as a source of energy and ketoleucine that can also be utilized in the liver, resulting in the production of ketone bodies.(29)

However, the comparison of our findings with previous studies on caloric restriction(30;31) reveals not only the resemblance but some important differences such as dissimilar changes in lactate, hippurate, succinate, and other compounds. Thus, metabolic phenotype of ERCC1$^{d/-}$ mice cannot be reduced to the caloric restriction but reflects a complex, systemic effect of a mutation.

The significantly increased level of citrate in urine of ERCC1$^{d/-}$ mice might point to metabolic alkalosis in these mice.(32) This supposition is strengthened by the fact that

glutamine, which is also related to maintaining acid-base balance,(33) was also found to be elevated in urine.

Kidney malfunction may be the reason for the decrease of hippuric acid secretion, which normally occurs through renal tubules. The decrease of taurine in urine, an important component of bile, as well as the decrease of allantoin in urine may reflect liver dysfunction.(34) Hepatic dysfunction might also be indicated by increased alanine in blood. Although pronounced kidney and liver dysfunctions develop in ERCC1$^{d/-}$ mice at a much older age (after 30 weeks), these compounds found in urine point at attenuated function of these organs already at an earlier age.

In conclusion, besides changes associated with malfunctions of some organs, the NMR data indicated that in ERCC1$^{d/-}$ mice a specific "survival" response is activated that primarily alters energy metabolism and leads to ketosis. These results are in line with the previous observations for the double knockout of ERCC1 gene in comparison to caloric restriction that showed almost identical changes in transcription and biochemistry mediated by insulin pathway.(8)

CONCLUSIONS

Using profiling by ^{1}H NMR and subsequent multivariate statistical analysis, differences in metabolic composition of both serum and urine between wild type and ERCC1$^{d/-}$ mice were found. Dependence of the profiles on age was clearly present, showing that a major change happened between 8 and 12 weeks in both of the genetically different classes of animals, which most probably reflects the time of their sexual maturity.

Differences in molecular composition assessed by NMR in serum and urine indicate a relative change of lipoproteins (decrease in LDL and VLDL, increase in HDL in mutants compared to controls), a shift of the energy metabolism to ketosis, as well as kidney and liver malfunction and possibly metabolic alkalosis in mutant mice.

REFERENCES

1. Kirkwood,T.B., and Austad,S.N. 2000. Why do we age? Nature 408:233-238.

2. Droge,W. 2002. Free radicals in the physiological control of cell function. Physiological Reviews 82:47-95.

3. Beckman,K.B., and Ames,B.N. 1998. The free radical theory of aging matures. Physiological Reviews 78:547-581.

4. Lehmann,A.R. 2003. DNA repair-deficient diseases, xeroderma pigmentosum, Cockayne syndrome and trichothiodystrophy. Biochimie 85:1101-1111.

5. Guarente,L., and Kenyon,C. 2000. Genetic pathways that regulate ageing in model organisms. Nature 408:255-262.

6. McWhir,J., Selfridge,J., Harrison,D.J., Squires,S., and Melton,D.W. 1993. Mice with DNA repair gene (ERCC-1) deficiency have elevated levels of p53, liver nuclear abnormalities and die before weaning. Nat. Genet. 5:217-224.

7. Niedernhofer,L.J., Odijk,H., Budzowska,M., van,D.E., Maas,A., Theil,A.F., de,W.J., Jaspers,N.G., Beverloo,H.B., Hoeijmakers,J.H. *et al* 2004. The structure-specific endonuclease Ercc1-Xpf is required to resolve DNA interstrand cross-link-induced double-strand breaks. Mol. Cell Biol. 24:5776-5787.

8. Niedernhofer,L.J., Garinis,G.A., Raams,A., Lalai,A.S., Robinson,A.R., Appeldoorn,E., Odijk,H., Oostendorp,R., Ahmad,A., van,L.W. *et al* 2006. A new progeroid syndrome reveals that genotoxic stress suppresses the somatotroph axis. Nature 444:1038-1043.

9. Weeda,G., Donker,I., deWit,J., Morreau,H., Janssens,R., Vissers,C.J., Nigg,A., vanSteeg,H., Bootsma,D., and Hoeijmakers,J.H.J. 1997. Disruption of mouse ERCC1 results in a novel repair syndrome with growth failure, nuclear abnormalities and senescence. Current Biology 7:427-439.

10. Dolle,M.E., Busuttil,R.A., Garcia,A.M., Wijnhoven,S., van,D.E., Niedernhofer,L.J., van der,H.G., Hoeijmakers,J.H., van,S.H., and Vijg,J. 2006. Increased genomic instability is not a prerequisite for shortened lifespan in DNA repair deficient mice. Mutat. Res. 596:22-35.

11. Fiehn,O. 2002. Metabolomics--the link between genotypes and phenotypes. Plant Mol. Biol. 48:155-171.

12. Holmes,E., Wilson,I.D., and Nicholson,J.K. 2008. Metabolic phenotyping in health and disease. Cell 134:714-717.

13. Lindon,J.C., and Nicholson,J.K. 2008. Analytical technologies for metabonomics and metabolomics, and multi-omic information recovery. Trac-Trends in Analytical Chemistry 27:194-204.

14. Nicholson,J.K., and Lindon,J.C. 2008. Systems biology: Metabonomics. Nature 455:1054-1056.

15. Trygg,J., Holmes,E., and Lundstedt,T. 2007. Chemometrics in metabonomics. Journal of Proteome Research 6:469-479.

16. Nicholson,J.K., Lindon,J.C., and Holmes,E. 1999. 'Metabonomics': understanding the metabolic responses of living systems to pathophysiological stimuli via multivariate statistical analysis of biological NMR spectroscopic data. Xenobiotica 29:1181-1189.

17. Findeisen,M., Brand,T., and Berger,S. 2007. A ^{1}H-NMR thermometer suitable for cryoprobes. Magn Reson. Chem 45:175-178.

18. Kumar,A., Ernst,R.R., and Wuthrich,K. 1980. A two-dimensional nuclear Overhauser enhancement (2D NOE) experiment for the elucidation of complete proton-proton cross-relaxation networks in biological macromolecules. Biochem. Biophys. Res. Commun. 95:1-6.

19. Wu,D.H., Chen,A.D., and Johnson,C.S. 1995. An Improved Diffusion-Ordered Spectroscopy Experiment Incorporating Bipolar-Gradient Pulses. Journal of Magnetic Resonance Series A 115:260-264.

20. Cloarec,O., Dumas,M.E., Craig,A., Barton,R.H., Trygg,J., Hudson,J., Blancher,C., Gauguier,D., Lindon,J.C., Holmes,E. *et al* 2005. Statistical total correlation spectroscopy: An exploratory approach for latent biomarker identification from metabolic H-1 NMR data sets. Analytical Chemistry 77:1282-1289.

21. Nielsen,N.P.V., Carstensen,J.M., and Smedsgaard,J. 1998. Aligning of single and multiple wavelength chromatographic profiles for chemometric data analysis using correlation optimised warping. Journal of Chromatography A 805:17-35.

22. Lindon,J.C., Nicholson,J.K., and Everett,J.R. 1999. NMR spectroscopy of biofluids. Annual Reports on Nmr Spectroscopy, Vol 38 38:1-88.

23. Schumacher,B., van,d.P., I, Moorhouse,M.J., Kosteas,T., Robinson,A.R., Suh,Y., Breit,T.M., van,S.H., Niedernhofer,L.J., van,I.W. *et al* 2008.

Delayed and accelerated aging share common longevity assurance mechanisms. PLoS. Genet. 4:e1000161.

24. van de Ven,M., Andressoo,J.O., Holcomb,V.B., von Lindern,M., Jong,W.M., De Zeeuw,C.I., Suh,Y., Hasty,P., Hoeijmakers,J.H., van der Horst,G.T. *et al* 2006. Adaptive stress response in segmental progeria resembles long-lived dwarfism and calorie restriction in mice. PLoS Genet. 2:e192.

25. Anderson,R.M., Shanmuganayagam,D., and Weindruch,R. 2009. Caloric restriction and aging: studies in mice and monkeys. Toxicol. Pathol. 37:47-51.

26. Robertson,D.G. 2005. Metabonomics in toxicology: A review. Toxicological Sciences 85:809-822.

27. Nicholson,J.K., Timbrell,J.A., and Sadler,P.J. 1985. Proton Nmr-Spectra of Urine As Indicators of Renal Damage - Mercury-Induced Nephrotoxicity in Rats. Molecular Pharmacology 27:644-651.

28. Mcgarry,J.D., and Foster,D.W. 1980. Regulation of Hepatic Fatty-Acid Oxidation and Ketone-Body Production. Annual Review of Biochemistry 49:395-420.

29. Harper,A.E., Miller,R.H., and Block,K.P. 1984. Branched-Chain Amino-Acid-Metabolism. Annual Review of Nutrition 4:409-454.

30. Rezzi,S., Martin,F.P., Shanmuganayagam,D., Colman,R.J., Nicholson,J.K., and Weindruch,R. 2009. Metabolic shifts due to long-term caloric restriction revealed in nonhuman primates. Exp. Gerontol. 44:356-362.

31. Wang,Y.L., Lawler,D., Larson,B., Ramadan,Z., Kochhar,S., Holmes,E., and Nicholson,J.K. 2007. Metabonomic investigations of aging and caloric restriction in a life-long dog study. Journal of Proteome Research 6:1846-1854.

32. Gordon,E.E. 1963. Effect of Acute Metabolic Acidosis and Alkalosis on Acetate Anc Citrate Metabolism in Rat. Journal of Clinical Investigation 42:137-&.

33. Taylor,L., and Curthoys,N.P. 2004. Glutamine metabolism - Role in acid-base balance. Biochemistry and Molecular Biology Education 32:291-304.

34. Wishart,D.S. 2005. Metabolomics: The principles and potential applications to transplantation. American Journal of Transplantation 5:2814-2820.

35. Kriat,M., Confort-Gouny,S., Vion-Dury,J., Sciaky,M., Viout,P., and Cozzone,P.J. 1992. Quantitation of metabolites in human blood serum by proton magnetic resonance spectroscopy. A comparative study of the use of formate and TSP as concentration standards. NMR Biomed. 5:179-184.

SUPPLEMENTARY MATERIALS

Table S1. Mean body weight, g (SD) of mice with different genetic background and at different ages.

Age, wks \ Genotype	Wild type	ERCC1d/-
8	23.7(4.1)	14.7(1.7)
12	25.7(5.3)	14.1(1.4)
16	26.0(6.1)	14.3(1.8)
20	30.3(7.5)	12.9(1.4)

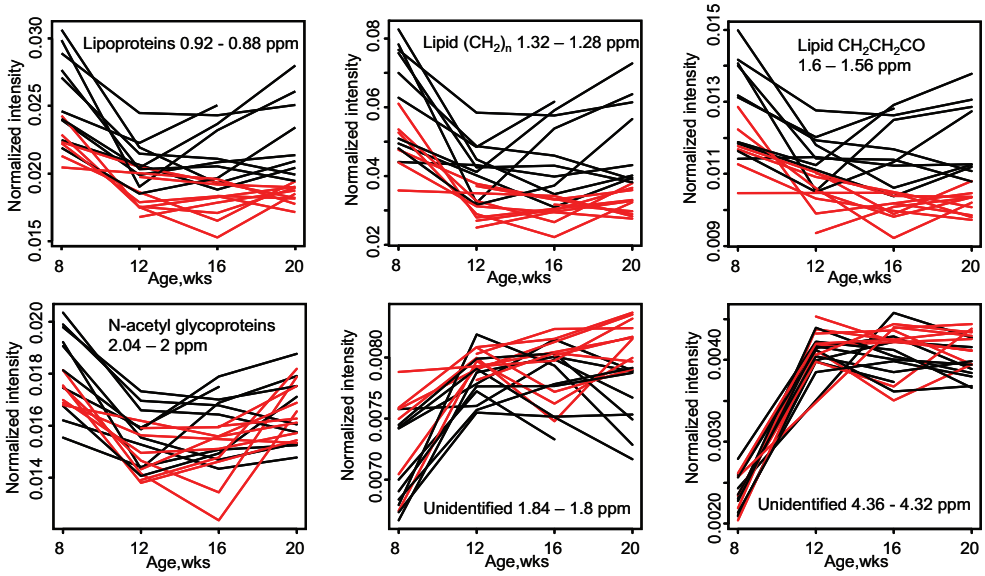

Figure S1. Metabolic compounds of serum related to age and their changes with age. Black lines represent changes in intensity of selected variables in wild type, red in ERCC1$^{d/-}$ mutants.

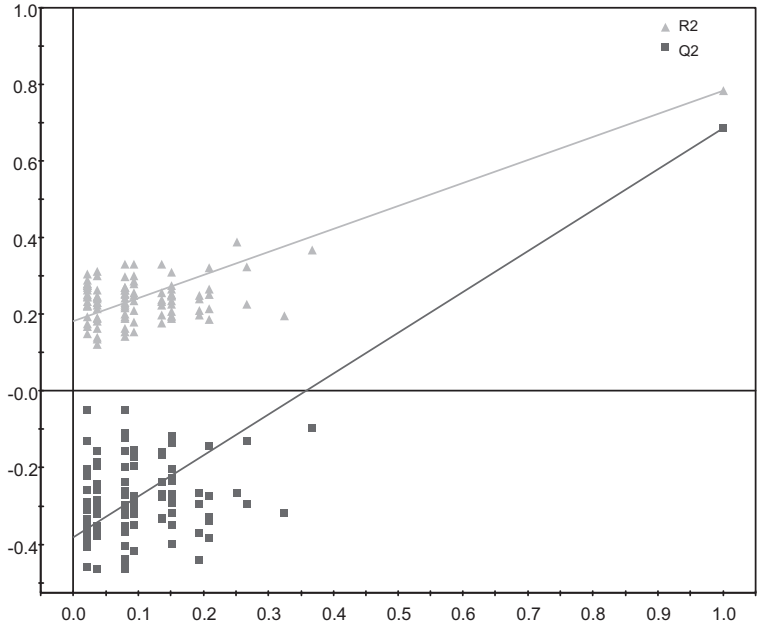

Figure S2. Validation plot of PLS-DA model for mouse serum NMR data with 100 permutations; squares show the Q^2 values and triangles are R^2 values.

Absolute Glucose Quantification. In general TSP and DSS are not suitable as reference for absolute metabolite quantification in serum and plasma due to their interaction with serum albumin which results in exchange broadening of the reference signal(35). However, for relatively similar plasma/serum samples (like metabonomics samples from individuals/animals collected under controlled conditions) a correction factor for the integral of the TSP signal can be calculated from comparison of samples with known TSP concentration in the presence and absence of serum/plasma. In first approximation assuming similar relaxation behavior between the metabolite in serum and free TSP, the metabolite concentration can then directly be calculated from the corrected TSP integrals in serum/plasma.

For determination of the TSP correction factor an additional sample of 150 L pooled rat serum with addition of 150 µl of 1.5 M phosphate buffer in H_2O/D_2O (90/10) at pH 7.4 containing 4% NaN_3 and 2 mM TSP was prepared. As reference for free TSP a second sample was prepared by adding 150 µl of 1.5 M phosphate buffer in H_2O/D_2O (90 /10) at pH 7.4 containing 4% NaN_3 and 2 mM TSP to 150 µl of 0.9% NaCl saline solution. Both samples were measured in 3mm NMR Match tubes using the first increment of a NOESY pulse sequence as described in the experimental section.

For quantification the deconvoluted TSP signals were used in order to avoid any interference with overlapping broad protein resonances in the case of the serum spectrum. The region between 0.2 and -0.2 ppm was baseline corrected automatically by subtraction of a 1st order polynomial removing any broad signals from proteins in this region. The TSP signal was then deconvoluted by fitting a mixed Lorentzian/Gaussian function (60/40) to the peak using the build-in MDCON command in Topspin (Version 2.1 pl4, Bruker Biospin). The parameters were adjusted for peak position and half width of the corresponding signal. The obtained deconvoluted signals were then quantified based on the area under the curve as determined by the MDCON algorithm. A correction factor of 1.93 for TSP in serum compared to saline was determined after correction for differences in nc_proc (Supplementary Materiaks, Figure S3).

Based on the determined correction factor, the absolute Glucose concentrations were calculated using the following formula:

$$c_G = \frac{I_G * C_T * H_T}{1.93 * I_T * H_G}$$

I_G : Integral -anomeric proton of Glucose

H_G: Number of protons of deconvoluted Glucose signal (0.36H assuming anomeric equilibrium – note only anomeric proton is used for quantification)

I_T: Integral TSP signal

H_T: Number of protons of deconvoluted TSP signal (9H)

C_T: Concentration of TSP in sample

Glucose concentrations in serum were calculated taking into account 4-time dilution of the serum sample with buffer .

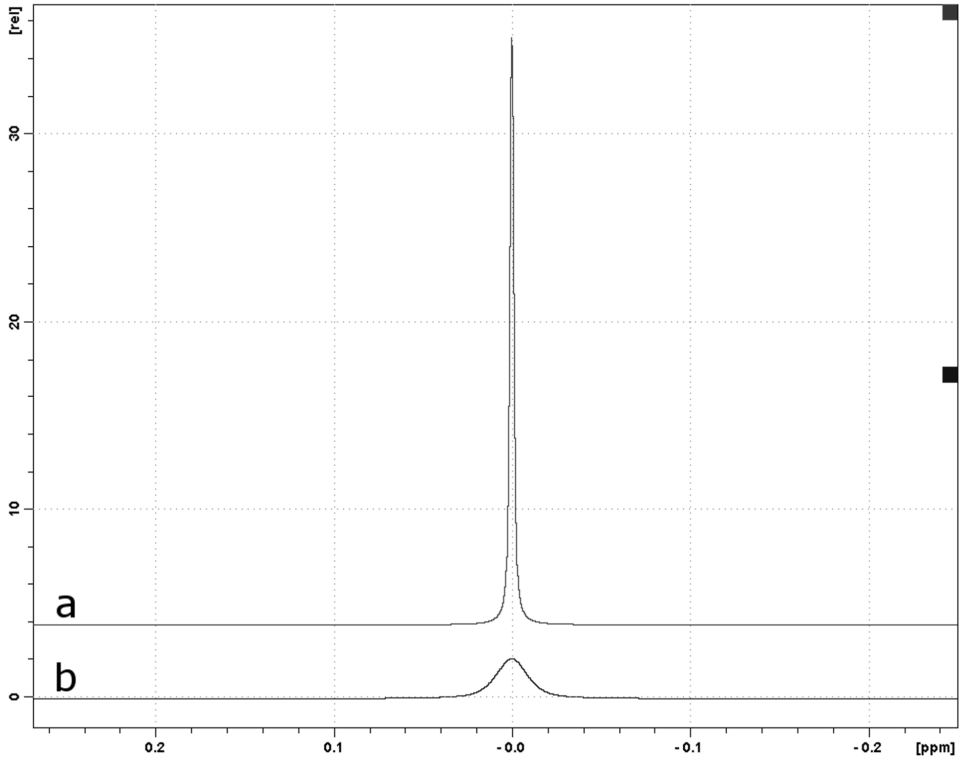

Figure S3. Comparison of deconvoluted TSP signal from (a) 1mM TSP in Saline/Buffer solution (line width = 1.5 Hz / integral = 378.5) and (b) 1 mM TSP in Serum/Buffer solution (line width = 12.4 Hz / integral = 196.0).

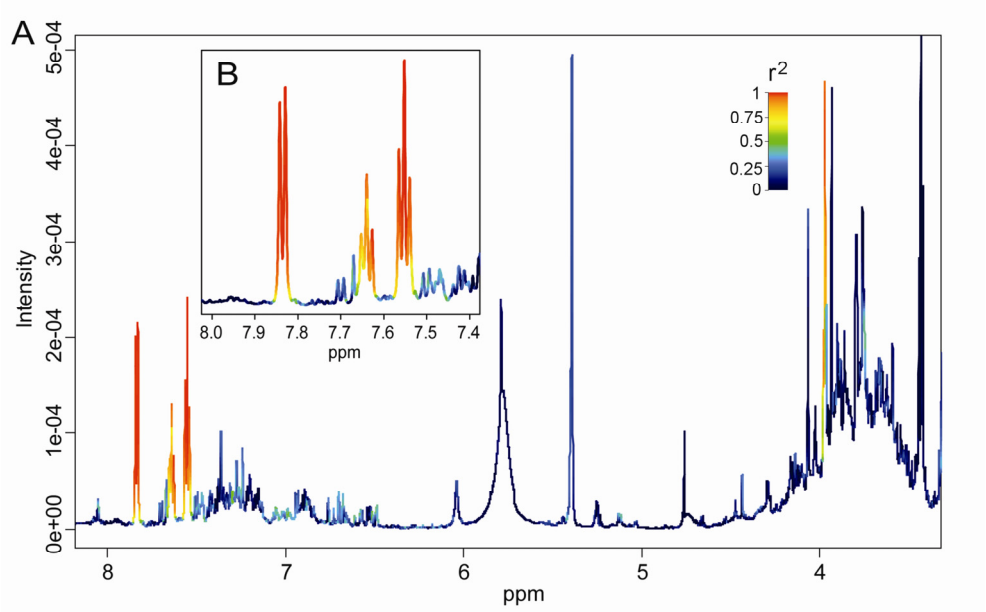

Figure S4. One-dimensional STOCSY analysis for the selected variable from the urine spectrum corresponding to 7.55 ppm. The degree of correlation across the spectrum has been color coded and projected on the spectrum that has the maximum for this variable. A) spectrum between 8 and 3.5 ppm B) zoomed in region between 8 and 7.4 ppm.

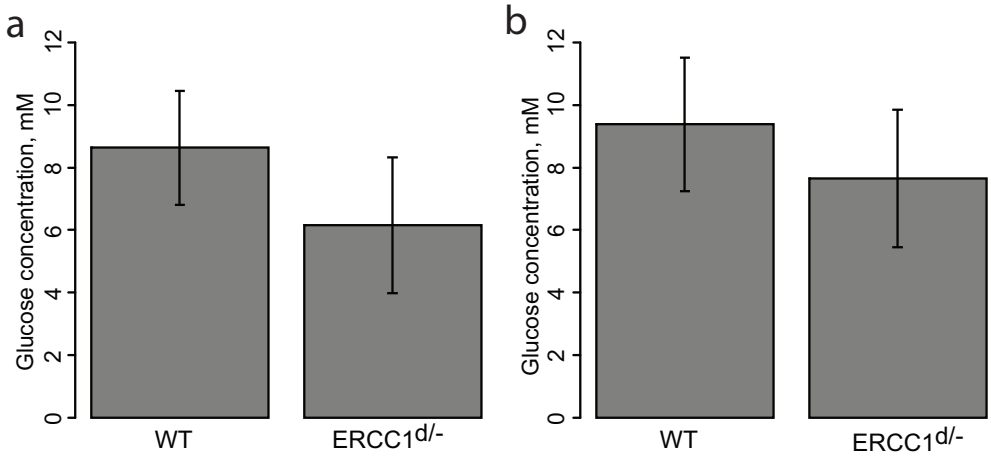

Figure S5. Glucose concentration in blood (a) measured by a conventional method (Freestyle mini blood glucose measurement device) (b) quantified based on NMR spectra. Error bars indicate standard deviations.

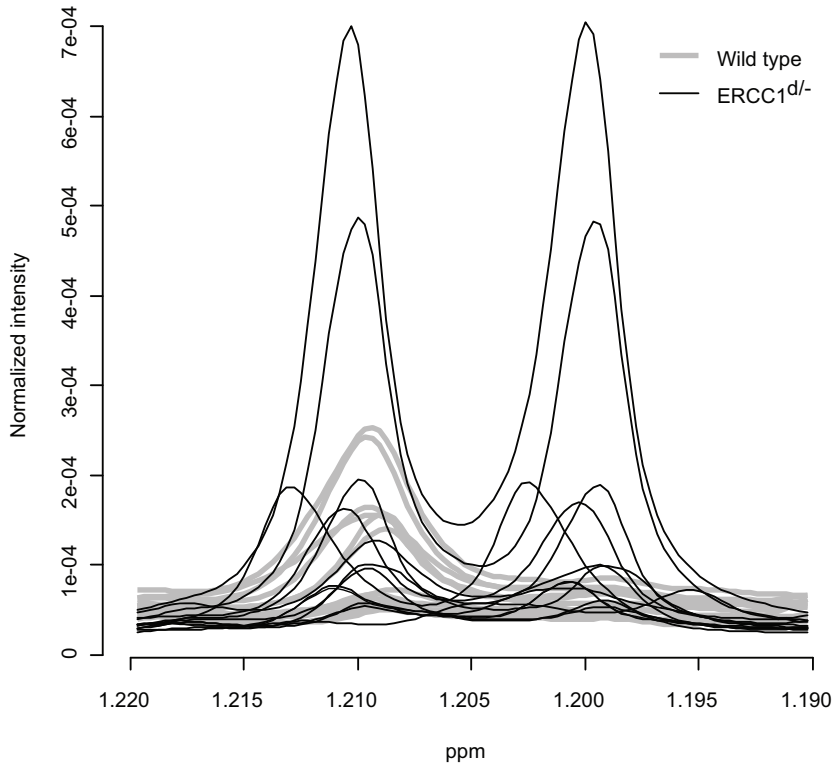

Figure S6. Spectral region of 3-hydroxybutyric acid doublet in urine samples, spectra from wild type animals are represented by black lines and from ERCC1$^{d/-}$ mutants by red lines.